

Review

# Functionalization of Fabrics with Graphene-Based Coatings: Mechanisms, Approaches, and Functions

Yang Liu <sup>1,\*</sup> , Bin Fei <sup>2</sup> and John H. Xin <sup>2,\*</sup><sup>1</sup> School of Biomedical Engineering, Sun Yat-sen University, Shenzhen 518107, China<sup>2</sup> School of Fashion and Textiles, The Hong Kong Polytechnic University, Hong Kong SAR 999077, China; bin.feii@polyu.edu.hk

\* Correspondence: liuyang56@mail.sysu.edu.cn (Y.L.); john.xin@polyu.edu.hk (J.H.X.)

**Abstract:** Due to their unique surface-active functionalities, graphene and its derivatives, i.e., graphene oxide (GO) and reduced graphene oxide (rGO), have received enormous research attention in recent decades. One of the most intriguing research hot spots is the integration of GO and rGO coatings on textiles through dyeing methods, e.g., dip-pad-dry. In general, the GO sheets can quickly diffuse into the fabric matrix and deposit onto the surface of the fibers through hydrogen bonding. The GO sheets can be conformally coated on the fiber surface, forming strong adhesion as a result of the high flakiness ratio, mechanical strength, and deformability. Moreover, multiple functions with application significance, e.g., anti-bacteria, UV protection, conductivity, and wetting control, can be achieved on the GO and rGO-coated fabrics as a result of the intrinsic chemical, physical, electronic, and amphiphilic properties of GO and rGO. On the other hand, extrinsic functions, including self-cleaning, self-healing, directional water transport, and oil/water separation, can be achieved for the GO and rGO coatings by the integration of other functional materials. Therefore, multi-scale, multifunctional, smart fabrics with programmable functions and functional synergy can be achieved by the design and preparation of the hybrid GO and rGO coatings, while advanced applications, e.g., healthcare clothing, E-textiles, anti-fouling ultrafiltration membranes, can be realized. In this review, we aim to provide an in-depth overview of the existing methods for functionalizing fabrics with graphene-based coatings while the corresponding functional performance, underlying mechanisms and applications are highlighted and discussed, which may provide useful insights for the design and fabrication of functional textiles and fabrics for different applications.

**Keywords:** graphene oxide; reduced graphene oxide; hybrid; coating; multifunctional

**Citation:** Liu, Y.; Fei, B.; Xin, J.H. Functionalization of Fabrics with Graphene-Based Coatings: Mechanisms, Approaches, and Functions. *Coatings* **2023**, *13*, 1580. <https://doi.org/10.3390/coatings13091580>

Academic Editor: Csaba Balázsi

Received: 26 July 2023

Revised: 21 August 2023

Accepted: 7 September 2023

Published: 11 September 2023



**Copyright:** © 2023 by the authors. Licensee MDPI, Basel, Switzerland. This article is an open access article distributed under the terms and conditions of the Creative Commons Attribution (CC BY) license (<https://creativecommons.org/licenses/by/4.0/>).

## 1. Introduction

Graphene-based materials, i.e., graphene oxide (GO), reduced graphene oxide (rGO), and graphene, have attracted significant research attention in decades due to their superior electrical, electronic, and mechanical properties [1–3]. According to the theoretical prediction, graphene, which is composed of a single layer of carbon basal plane, would have the highest conductivity and strength among the existing materials [4]. A schematic illustration of the graphene structure can be seen in Figure 1. In general, graphene is obtained through an irreversible reduction of its precursor, graphene oxide (GO), either through a chemical, thermal, or electrochemical method [5]. However, the full reduction of GO to graphene is experimentally hard, and rGO with various degrees of defects and oxygen vacancies is generally obtained. Chemical reduction, electrochemical exfoliation, and mechanical exfoliation are widely used to synthesize rGO [6–8], while UV irradiation and thermal reduction can be applied to obtain functionalized rGO from GO [9,10]. As a result of the unique properties of graphene, it has raised a busting wave for exploring its potential electronic, mechanical, and chemical applications, as shown in Figure 2. Integrated circuits based on graphene have been created by IBM, which demonstrated the possibility of the

next-generation electronics going beyond silicon and metals [11]; dual-gated graphene-based ambipolar amplifiers capable of operating in both the common and differential modes have been developed, showing remarkable potential in the low-noise-circuit application [12]. The impermeable atomic membrane of graphene has been fabricated, which inhibited the penetration of standard gases, including helium, but is readily permeable to water vapors [13]; graphene-based fibers, fabrics, and textiles have also emerged with high conductivity and flexibility, providing feasible solutions for the fabrication of smart, stimuli-responsive textiles [14–16].

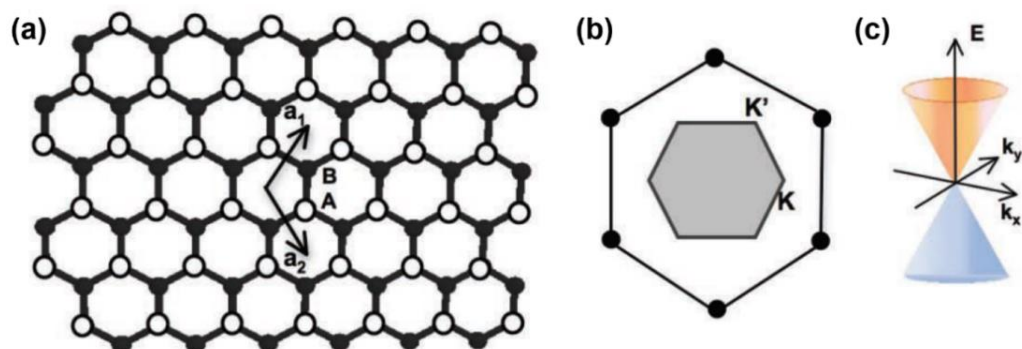


**Figure 1.** (a) Crystal structure, (b) Brillouin zone, and (c) band dispersion at a Dirac point of graphene. In (a), the Bravais lattice structure of graphene is consisting of two carbon atoms, which are drawn as white and black circles, and labeled as A and B, respectively. The arrows  $a_1$  and  $a_2$  represent the primitive lattice vectors with lengths equal to the lattice constant. In (b), the outer hexagonal ring represents the reciprocal lattice of graphene, and the inner shaded area represents the first Brillouin zone,  $K'$  and  $K$  indicate the non-equivalent corners. In (c), the coordinate axes  $k_x$  and  $k_y$  represent the  $k$ -space basis vector, and energy ( $E$ ) is the  $z$ -axis. Reproduced from ref. [1], with permission from Wiley, 2010.

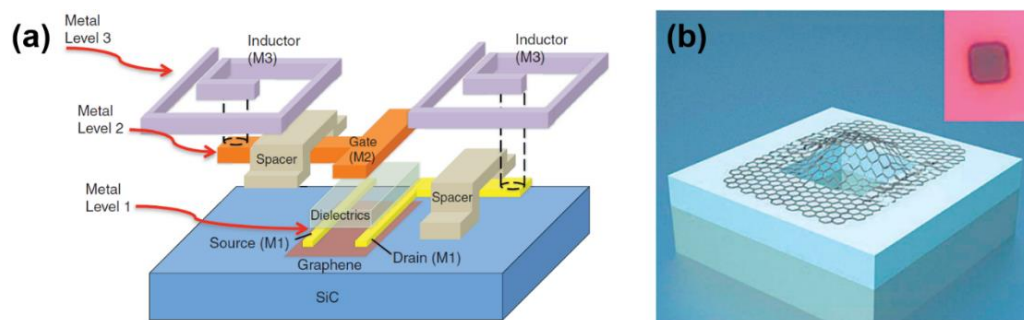


**Figure 2.** (a) Illustration of a graphene mixer circuit with a top-gated graphene transistor and two inductors connected to the gate and drain of the transistor. Reproduced from ref. [11], with permission from The American Association for the Advancement of Science, 2011. (b) Illustration of a graphene-sealed microchamber and optical image of a single atomic thick graphene drumhead on 440 nm  $\text{SiO}_2$ . Reproduced from ref. [13], with permission from The American Chemical Society, 2008.

On the other hand, as the indispensable precursor of graphene, GO has also become a hot spot of research. However, GO has a similar molecular structure to graphene, which is also generally composed of a few graphene layers, except that functional groups, such as hydroxyl, epoxide, carbonyl, or carboxylic groups, are distributed on the basal planes along with distorted aliphatic regions due to harsh oxidizing reactions [17], though the actual structure can be more complicated and case-dependent. A proposed structure of GO can be seen in Figure 3. In addition, as a result of the hydrophilic functional groups and heterogeneous molecular structure, GO exhibits excellent amphiphilic properties as it can be readily dispersed in either aqueous or common organic solvents or assists the

dispersion of other carbon materials, which can be defined as a “surfactant” [18–20]. The functional groups of GO have also enabled the chemical functionalities of the material. Chemical functionalization, either covalently or non-covalently, has been applied to GO, and functional branches, such as aliphatic amines, polymers, and organosilanes, were attached to GO planes for enhanced non-aqueous dispersibility, tunable gas permeability, and composite forming properties [21–24]. It is also noteworthy that GO can serve as the catalyst for the oxidation of aromatic alcohols, alkenes, and Suzuki–Miyaura coupling reactions, which is then termed “carbocatalysis” [25]. According to these inspiring findings, the catalytic activity of GO can be quite broad, and the usage of this large-surface-area, non-metallic catalyst is very attractive for both industry and environmental protection [26].

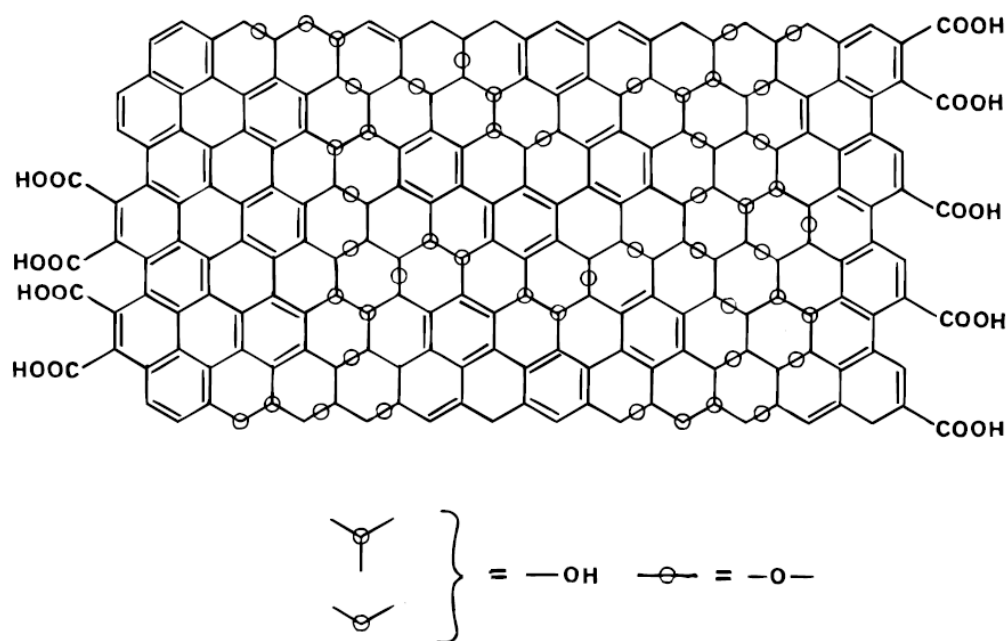


**Figure 3.** Schematic illustration of the structure of GO based on the Lerf–Klinowski model. Reproduced from ref. [17], with permission from The American Chemical Society, 1998.

Based on the intrinsic properties of GO and rGO, it is not hard to imagine their impact on the functions of traditional fibers and textiles. By integrating GO and rGO into the conventional dyeing and finishing process, unique and new functions and applications can be anticipated.

## 2. Functionalization of Fabrics Using Graphene Based Coatings: The Concept and Mechanism

Recently, the integration of textiles with GO has attracted much research attention, and the research significance may span across a wide range of applications, e.g., moisture and thermal management, biomedical, E-textiles, and oil–water separation [27–31]. In fact, GO and rGO have been applied to traditional fibers and fabrics using various methods, including dip-coating, filtration, dip-pad-dry-curing, pad-drying, and dyeing [32–36]. Intriguing functions, such as anti-bacterial, photocatalytic, electrocatalytic, and enhanced thermal stability, are obtained through the GO coatings on the fabrics [37–39]. Furthermore, the immobilized GO on the fabrics can be readily converted to rGO, which endows the base fabric with a conductive pathway and electrical property. By reducing GO on the as-obtained fabric, conductivity ranges from  $102\text{--}1010\ \Omega\ \text{cm}^{-1}$  can be achieved for fabrics composed of insulating fibers, such as acrylics and cotton [32,36]. rGO-coated nylon-6 fabrics with conductivity larger than  $1000\ \text{S}\ \text{m}^{-1}$  have also been fabricated with the assistance of bovine serum albumin (BSA) [40]. On the other hand, the rGO-coated cotton fabric showed remarkable thermoelectric properties when an additional coating layer of

PEDOT:PSS was applied, forming a wearable thermoelectric generator [41]. Moreover, the thermal conductivity of cotton fabric can be significantly enhanced by both the GO and rGO coatings. A. Kumar et al. investigated the thermal conductivity of polyethylene glycol (PEG) grafted cotton fabric coated by GO, and the result indicated a 10-fold increase in thermal conductivity for the GO-coated PEG-grafted fabric [0.52 W/(m · K)] as compared to the bare cotton fabric [0.045 W/(m · K)] [42]. G. Manasoglu et al. have reported the fabrication of rGO-coated polyester fabric by using a knife-over-roll technique, and the thermal conductivity of the polyester fabric can be increased from 0.10 up to 0.42 W/(m · K) by applying the rGO coating [43].

Though substantial attempts have been made to apply graphene-like materials on the fabrics, there are still many concerns and issues that exist for their practical applications. One of the major problems is that only dull brown or black colors can be obtained by dyeing fabrics with GO or rGO, respectively. In addition, due to the adsorption of GO on the fabric, the intrinsic dyeing sites on the fabrics are hindered, which means the color of the fabric is hard to adjust or change by the subsequent dyeing process. However, color is one of the most important factors that affect the customer's choice against textile products, i.e., fabrics, apparel, and fibers. The unresolved color issue associated with the GO or rGO-modified fabrics may generate a negative impact and hinder their further application in commercial textiles. The possibility of dyeing the fabrics with GO while retaining color control has opened a new path to integrate graphene-like materials with textiles. Typical colors and appearance of the GO and rGO coated fabrics are shown in Figure 4.

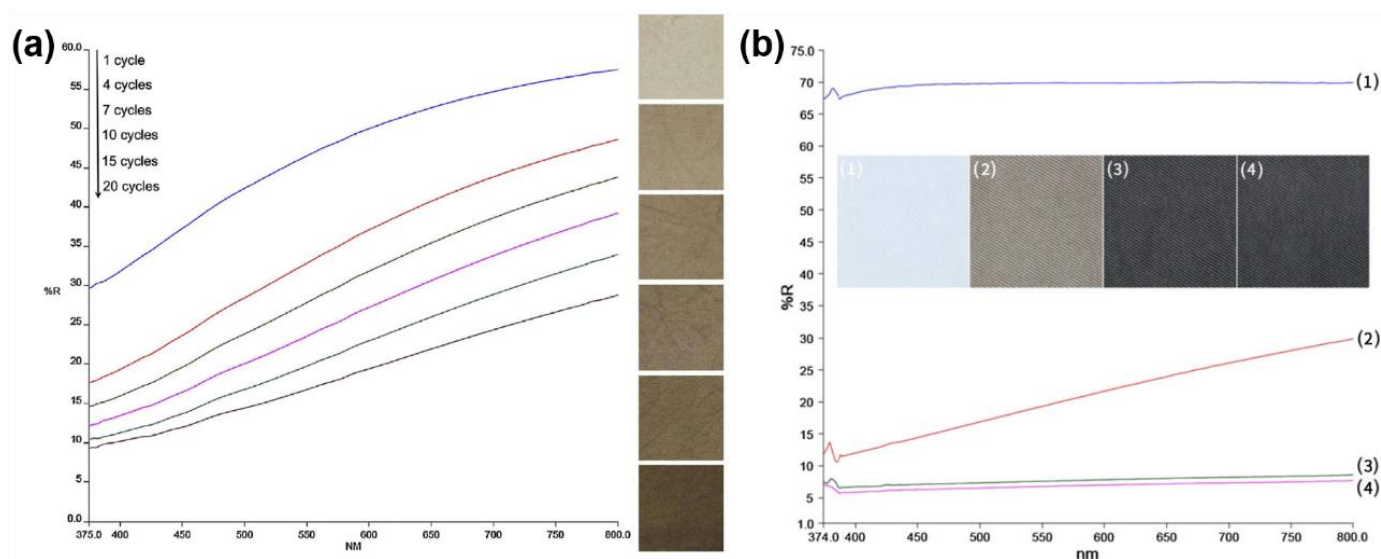


**Figure 4.** (a) Reflectance spectra and the corresponding optical images of the GO-coated cotton fabrics with different dip-drying cycles. Reproduced from ref. [32], with permission from Elsevier, 2013. (b) Reflectance spectra and the corresponding optical images of cotton, GO-coated cotton, rGO-coated cotton, and polymethyl siloxane-rGO-coated cotton fabrics (from 1–4). Reproduced from ref. [34], with permission from Springer, 2013.

Dyeing fabrics with GO may depend on the good water dispersibility of GO and its intrinsic molecular structure. The dye molecules can non-covalently bond to the GO sheets via the strong  $\pi$ - $\pi$  interaction between the large aromatic rings, forming a stable GO-dye molecular complex [44]. Subsequently, the GO-dye complex can migrate and immobilize the fabric through either chemical reactions or van der Waals forces. As a result, colors are obtained on the fabrics via the dyes, and at the same time, GO is also immobilized. Moreover, the surface of the fabric can be cationized by chemical modification in order to enhance the fabric-GO interactions through the electrostatic interaction. Besides the eye-catching colors endowed by the dyes, the immobilized GO can provide the fabric with

programmable functions through the post-functionalization processes. For example, facile anti-bacterial properties can be provided by the GO coating on cotton and linen fabrics, and the anti-bacterial property can be substantially enhanced by reducing the GO into rGO and depositing Ag nanoparticles on the rGO surface [45]; enhanced UV protective and photocatalytic properties, i.e., spontaneous and fast photodegradation of stains and dirt, can be obtained by the deposition of photocatalytic nanoparticles on the GO or rGO surface [46,47]; stimuli-responsive wettability, e.g., the wetting transition from hydrophobic to hydrophilic, can be achieved by sonicating the rGO-coated fabric in water [48]; reversible wetting transition from superhydrophobic to superhydrophilic can be realized on cotton fabrics by irradiating the hierarchical graphene/titania coating with UV light, and the fabric may gradually restore its superhydrophobicity during dark storage [49].

### 3. Functionalization of Fabrics Using Graphene Based Coatings: Applications

#### 3.1. Anti-Bacteria

Fabrics can obtain excellent anti-bacterial properties by integrating with GO. It is believed that GO can affect the bacteria metabolism and inhibit further growth of the bacteria in the environment. Cotton fabrics coated with GO showed high deactivation efficiency to both gram-negative and gram-positive bacteria, whereas no significant skin irritations were observed [50]. J. Zhao et al. have investigated the anti-bacterial effect of cotton fabrics coated by GO. In their study, GO was coated on the cotton fabrics by suction filtration (denoted as Cotton-GO), which can be subsequently crosslinked with the fabric by either  $\gamma$ -ray radiation or heating by using triallyl isocyanurate (TAIC) as the crosslinker [51]. All of the GO-coated fabrics showed remarkable anti-bacterial properties against both the gram-negative (*E. coli*) and gram-positive (*B. subtilis*) bacteria, as the colony-forming units generated by the eluents washed off from the GO-coated fabrics were much fewer than the ones generated by the eluents obtained from the bare cotton fabric (Figure 5a), and inhibition efficiencies around 98% can be obtained after incubating the bacteria with the GO-coated cotton fabrics (Figure 5b,c). Moreover, the GO-coated cotton fabrics can retain inhibition efficiencies higher than 90% after laundering 100 times. Compared to other newly-emerged anti-bacterial nanomaterials, GO has its intrinsic advantages as it can conformally wrap around the fiber surface, forming strong entanglements with the fabric substrate, which in turn provides superior wash fastness for the GO coatings. This feature cannot be obtained from materials such as carbon nanotubes, titanium dioxide, or silver nanoparticles, as they usually formed several microns-thick layers on the fabric, and the structures were hard to maintain due to the low abrasion resistance of the coatings [52]. F. Yaghoubidoust et al. investigated the anti-bacterial properties of the GO-coated cotton fabrics prepared by dip-coating, and different results were obtained as compared to the previous work [53]. The highest inhibition efficiency for *E. coli* was measured to be ~70% after 24 hours' incubation, while an inhibition efficiency as high as 93% was measured for the gram-positive *S. iniae* under the same condition. However, the prominent difference in the anti-bacterial properties of the GO-coated cotton fabrics in different studies may arise from the differences in the surface chemical and physical characteristics of the as-synthesized GO. N. Yadav et al. have shown that GO may inhibit the growth of both the gram-negative (*E. coli*) and gram-positive (*Staphylococcus aureus*) bacteria, and the inhibition efficiency was affected by the surface functional groups, size, and surface roughness of the as-prepared GO. However, a higher inhibition efficiency of the gram-negative bacteria was observed on the GO-coated surface in their study [54].

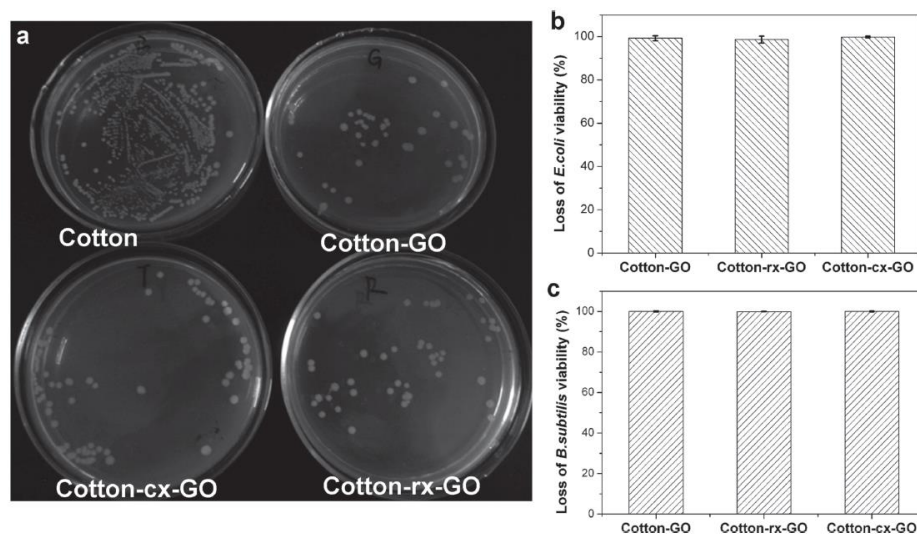


**Figure 5.** Anti-bacterial properties of the GO-coated cotton fabric. (a) Colonization of *E. coli* from the eluents washed off from the *E. coli* incubated GO-coated cotton fabrics on agar plates incubated for 18 h. (b) Inhibition efficiency of the GO-coated cotton fabric against *E. coli* and (c) *B. subtilis*. Cotton-GO, cotton-cx-GO, and cotton-rx-GO mean the cotton fabrics coated with GO by physical adsorption, chemical crosslinking with TAIC, and  $\gamma$ -ray-radiation crosslinking with TAIC, respectively. Reproduced from ref. [51], with permission from Wiley, 2013.

The GO coated on cotton fabrics can be further transformed into rGO by reduction. Compared to the GO-coated cotton fabric, the anti-bacterial property of the rGO-coated fabric may deteriorate while its electrical conductivity, UV absorption, and hydrophobicity can be significantly enhanced. The anti-bacterial mechanisms of GO and rGO against *E. coli* have been investigated by S. Liu et al. [50]. According to their findings, the GO dispersion showed the highest inhibition efficiency against *E. coli* among the tested carbon allotropes, i.e., graphite, graphite oxide, GO, and rGO (Figure 6a). The anti-bacterial properties of GO and rGO were time- and concentration-dependent, in which GO surpassed the performance of rGO (Figure 6b,c). This phenomenon can be attributed to the small particle sizes and narrow particle size distribution of the GO dispersion, which may provide a higher surface-to-volume ratio and enhance the interaction between GO and *E. coli*. On the other hand, destruction of the cell membranes was observed for the *E. coli* cells in contact with the GO and rGO nanosheets; oxidation of glutathione, a redox state mediator in bacteria, was observed for both GO and rGO. It thus revealed that the anti-bacterial mechanism of GO and rGO may involve both the membrane stress and oxidation stress pathways. U. Mizerska et al. have reported the fabrication of rGO-coated cotton fabrics by a pad-dry-anneal method, which utilized a mixture solution of GO, organosilicon sol, and surfactant as the coating solution [55]. The as-obtained rGO-coated cotton fabrics showed no inhibition zones against the tested bacteria (*E. coli* and *S. aureus*) on the inoculated agar plates. However, impeded biofilm formation can be observed on the surface of the rGO-coated cotton fabric as compared to the surface of the bare cotton fabric, where continuous bacterial biofilm formation can be observed. To further enhance the anti-bacterial properties of the rGO-coated cotton fabric, tert-butylamine or N,N-dimethyl-N-n-octylammonium groups can be introduced and attached to its surface, and the colonization of *E. coli* and *S. aureus* can be significantly reduced on the fabric surface. Z. Xu et al. reported the fabrication of coated cotton fabrics with high anti-bacterial efficiencies by using rGO and an N-halamine-containing quaternary ammonium salt (QAS), which showed inhibition efficiencies of ~80% and ~65% against *S. aureus* and *E. coli*, respectively [56]. Upon further chlorination of the rGO/QAS coated fabrics, the anti-bacterial efficiencies can be enhanced to 100%. Other than QAS, rGO can be integrated with metallic nanoparticles (NPs) to enhance the anti-bacterial properties and hydrophobicity. For example, J. Kim et al. fabricated a rGO/Cu NPs coating

on cotton fabrics, which showed high inhibition efficiencies (~99%) against *E. coli*, *C. xerosis*, and *M. luteus*, and no cytotoxicity effects against human skin cells were observed [57]. B. Jafari et al. reported the fabrication of anti-bacterial coatings on rayon/polyester blended fabrics by using rGO and Ag NPs. The fabric was first coated by GO through dip-coating, and subsequently, the reduction of GO and the deposition of Ag NPs were implemented through the chronoamperometric technique [58]. The rGO/Ag NPs coated fabrics showed excellent anti-bacterial properties and hydrophobicity, as an inhibition efficiency of 99.99% against *E. coli* and a WCA of 148° were obtained. D. P. Rodrigues et al. investigated the anti-bacterial properties of monolayer and few-layer rGO coated on polyamide fabrics [59]. They found that the monolayer rGO-coated fabrics showed no inhibition effects on *E. coli* and *S. aureus*, while the few-layer rGO-coated fabrics showed a concentration-dependent anti-bacterial effect. They also found that the addition of different dopants may change the electronic structure and surface polarity of rGO, resulting in either promotion or inhibition of the bacteria growth, which can be used to interpret the variations observed in different rGO-based coating methods and materials.

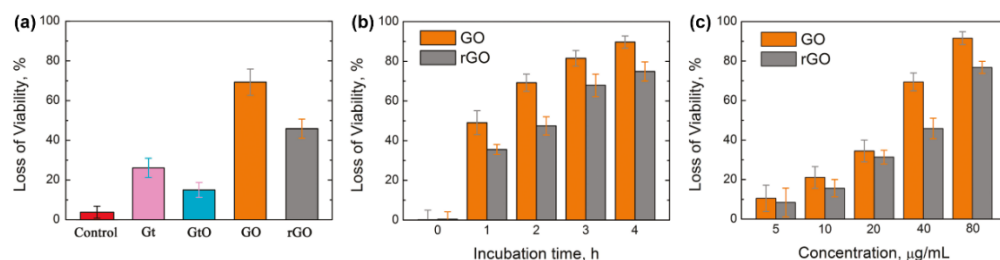


**Figure 6.** (a) Cell viability of *E. coli* after incubation with graphite (Gt), graphite oxide (GtO), graphene oxide (GO), and reduced graphene oxide (rGO) dispersions with a concentration of 80 µg mL<sup>-1</sup> and an incubation time of 2 h. (b) Time-dependent and (c) concentration-dependent cell viabilities of *E. coli* were obtained by incubating *E. coli* with GO and rGO dispersions with a fixed concentration (80 µg mL<sup>-1</sup>) and incubation time (2 h), respectively. Reproduced from ref. [50], with permission from The American Chemical Society, 2011.

### 3.2. UV Protection and Photocatalyst

Besides anti-bacterial properties, the GO-coated fabrics may show remarkable UV-protection properties that exceed the existing commercial anti-UV products. This feature can be ascribed to the unique electronic structure of GO, which is majorly composed of sp<sup>2</sup> hybridized carbon atoms. The transition from π to π\* orbitals of the GO π electrons can be excited by lights that have wavelengths in the UV range. Compared to graphite, which is almost UV transparent, GO typically shows an adsorption maximum at the wavelength ~230–300 nm [60,61], which can be seen in Figure 7a. Compared to GO, rGO may show an absorption maximum that shifts to higher wavelengths due to its more perfect sp<sup>2</sup> hybridized carbon structure [62], as shown in Figure 7b. X. He et al. have reported the fabrication of GO-coated cotton fabric by a simple dip-dry process [63]. In their study, the highest ultraviolet protection factor (UPF) measured for the GO-coated cotton fabrics was around 53, and the UPF increased as the concentration of GO and the times of the coating process increased. To enhance the UV protection and durability of the GO coating, D. Zuo et al. used ZnO quantum dots as photoactive additives and applied the hybrid coating layer of ZnO/GO/PVA on the cationized cotton fabric [64]. The UPF of the ZnO/GO/PVA coated cotton fabric can reach 61.3, which can be graded excellent according to the Australian/New Zealand standard (AS/NZS 4399). Moreover, a UPF of 57.6 was measured for the ZnO/GO/PVA coated fabric after washing 20 times, indicating the good wash fastness of the coating. B. C. Gültekîn reported the fabrication of GO-coated nonwoven cotton fabrics by using a simple dip-dry method, and rGO-coated fabrics can be obtained by the subsequent reduction of GO by sodium dithionite [65]. Both the GO and rGO-coated cotton fabrics showed UV-protective characteristics with UPF > 40

when the basis weight of the fabric exceeded  $70 \text{ g m}^{-2}$ . However, only the rGO-coated fabrics can achieve  $\text{UPF} > 50$  as the basis weight exceeds  $60 \text{ g m}^{-2}$ , indicating a better UV-protective property (Figure 7c). The rGO coating on the cotton fabric also showed excellent durability against washing, as  $\text{UPF} > 50$  was maintained for the coated fabrics after a standard washing durability test (ISO 105-C06-A1S).

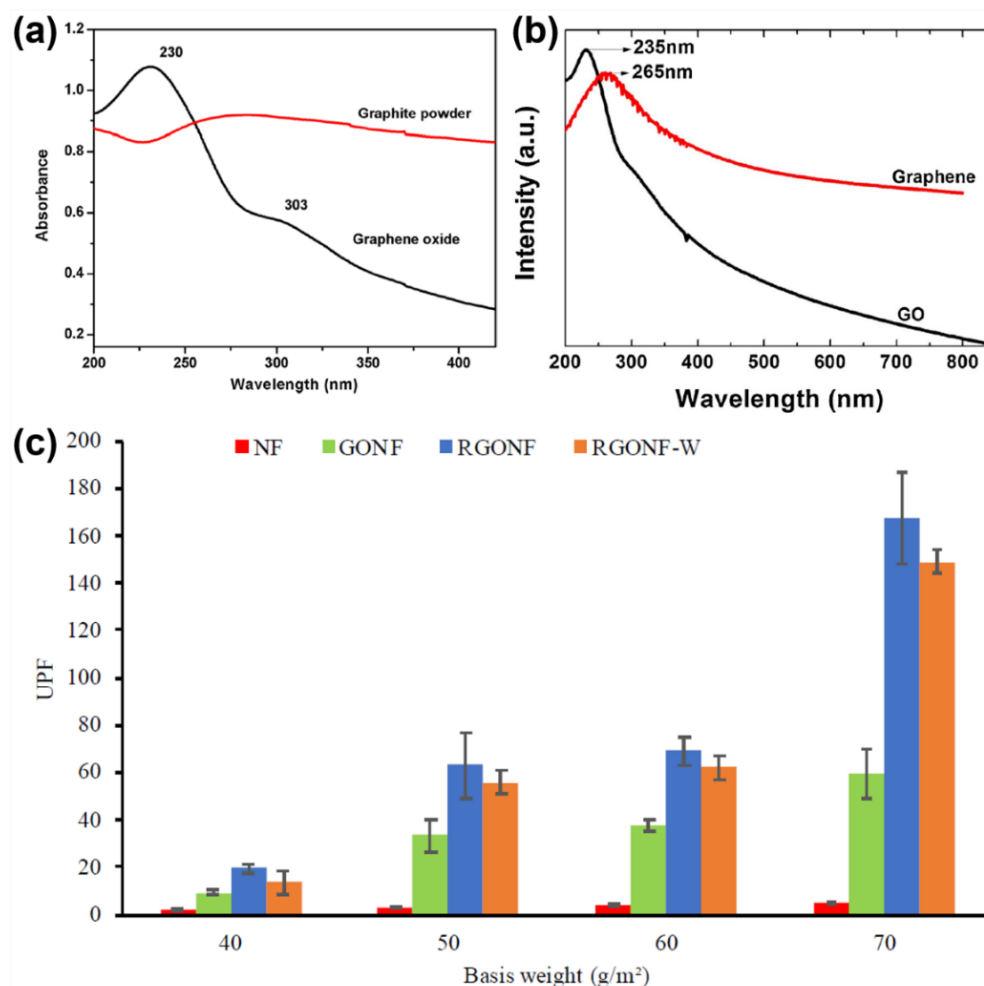


**Figure 7.** (a) UV spectra of graphene oxide and graphite powder. Reproduced from ref. [61], with permission from Springer, 2017. (b) UV-vis spectra of graphene and graphene oxide (GO). Reproduced from ref. [62], with permission from Elsevier, 2014. (c) UPF values of the bare nonwoven cotton fabric (NF), GO-coated nonwoven cotton fabric (GONF), rGO-coated nonwoven cotton fabric (RGONF), and rGO-coated nonwoven cotton fabric after the washing test. Reproduced from ref. [65], under the license of CC-BY 4.0.

Moreover, H. Zhao et al. utilized an electrophoretic deposition (EPD) method to graft GO on a polyethyleneimine (PEI) modified polyamide fabric's surface [66]. An intact and uniform GO coating layer with controllable surface morphology and thickness can be formed on the modified polyamide fabric's surface by EPD (Figure 8), and excellent UV-protective properties, electrical conductivity, and thermal conductivity were observed for the coated fabric as GO was converted to rGO by reduction. S. Bhattacharjee et al. reported the fabrication of rGO/Cu NPs and rGO/Ag NPs coatings on cotton fabrics by using 3-glycidylpropyl trimethoxy silane as a coupling agent [67]. The as-obtained rGO/Cu NPs coated fabrics showed excellent UV protective properties, low surface resistance, and high water contact angles (WCA).

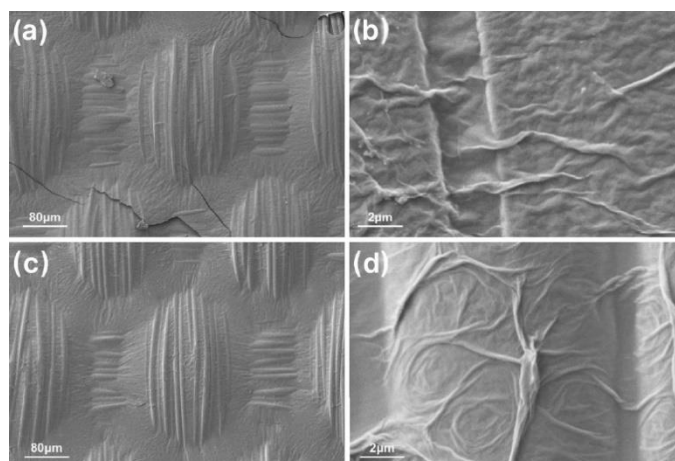


**Figure 8.** SEM images showing the surface morphologies of the graphene oxide coated, PEI grafted polyamide fabrics prepared by different EPD conditions: (a,b)  $0.5 \text{ mg mL}^{-1}$  GO suspension,  $10 \text{ V cm}^{-1}$  electric field strength, 90 s deposition time; (c,d)  $0.5 \text{ mg mL}^{-1}$  GO suspension,  $10 \text{ V cm}^{-1}$  electric field strength, 150 s deposition time. Reproduced from ref. [66], with permission from Springer, 2018.

As a result of its high photoactivity, GO can also be utilized as an easily accessible photocatalyst for many photo-conversion and redox processes due to its unique molecular configuration and tunable electronic structure [68–71]. It has been reported that GO can serve as the active redox mediator for accelerating the water-splitting reaction [72]. Moreover, GO can be used as the major photoactive component to catalyze the photo-splitting of xylose and xylan under visible light [73]. Due to its excellent chemisorption properties and the ability to activate oxygen species, there is increasing interest in the use of GO as a photocatalyst to remove organic contaminants and heavy metal ions [74,75]. Common organic compounds, such as methylene blue, rhodamine B, and phenol, can be photocatalyzed by GO or rGO-based materials, leading to either photodegradation or photoreduction, respectively [76–78]. The photocatalytic properties of GO can be further extended by the incorporation of other photoactive materials, such as metal oxides, quantum dots, and semiconductor nanostructures [79].

### 3.3. Tunable Superwettability and Separation Property

Compared with rGO, GO is intrinsically amphiphilic as a result of the difference in chemical composition in its edge region and basal plane. The edge region of GO is intrinsically more hydrophilic due to the enrichment of the oxygen-containing functional groups, e.g., carboxyl and hydroxyl [80]; on the contrary, the basal plane of GO is intrinsically more hydrophobic since C–C covalent bonds are dominated [81]. By manipulating the amphiphilic property of GO, the wettability of the fabric surface can be easily tuned from hydrophilic to hydrophobic by controlling the architecture of the GO coating. N. D. Tissera et al. have reported the fabrication of hydrophobic GO coating on a cotton fabric surface using a dyeing method [82]. According to their method, GO was coated onto the cotton fabric through a dip-pad-dry process, and a long dipping time was implemented to ensure the uniform deposition of GO on the fabric surface. Interestingly, the wettability of the GO-coated fabric surface can be tuned from hydrophilic with a WCA of  $60^\circ$  to hydrophobic with a WCA of  $143^\circ$  by simply altering the concentration of the GO dispersion used during the coating process. It was found that the GO nanosheets showed concentration-dependent morphologies and sizes in the dispersion, as thicker and larger nanosheets were observed in the dispersion with a high GO concentration (Figure 9A), and thinner and smaller nanosheets were observed in the dispersion with a low GO concentration (Figure 9B). The GO-coated cotton fabric showed an adhesive-type hydrophobicity, which can be attributed to the stacking of the basal planes of the GO

nanosheets and penetration of the water molecules to the underneath cotton fabric through the water channels formed by the edge region [83]. Upon further reducing GO into rGO, the hydrophobicity of the GO-coated fabric can be significantly enhanced. G. Cai et al. have reported the fabrication of GO-coated cotton fabric by using a dip-dry method [84]. However, the as-obtained GO-coated cotton fabric showed unstable hydrophobicity as the cast water droplet could be gradually absorbed by the fabric substrate. This problem was resolved by further reducing the GO coating into rGO coating through thermal treatment. Compared to the GO-coated fabric, the rGO-coated fabric showed stable hydrophobicity with a WCA of around  $125^\circ$  and a WCA of  $110^\circ$  can be maintained after eight washing cycles of the accelerated laundering tests (AATCC 61-2006). U. Mizerska et al. also reported the fabrication of rGO-coated cotton fabrics by thermally reducing the GO-coated cotton fabrics. However, the as-obtained hydrophobic rGO-coated cotton fabric ( $WCA \approx 143^\circ$ ) quickly became hydrophilic after sonicating in an aqueous solution of sodium dodecyl sulfate [85]. This phenomenon can be attributed to the chemisorption of the water molecules to the defect sites of the rGO basal planes [48]. To obtain robust superhydrophobic coatings on the surface of the cotton fabrics, an organosilicon sol was mixed with the GO dispersion to formulate a new coating recipe, which was subsequently applied to the cotton fabric by a dip-dry process. The rGO/organosilicon coating obtained after thermal reduction showed superhydrophobicity on the cotton fabric surface with a WCA of  $153^\circ$ , which was almost unchanged after the sonication treatment [85]. Other than cotton fabrics, the rGO coating can induce hydrophobicity on a wide range of woven or nonwoven porous substrates, such as polyethylene terephthalate (PET) fabrics, polypropylene membranes, and polyurethane membranes [86,87].

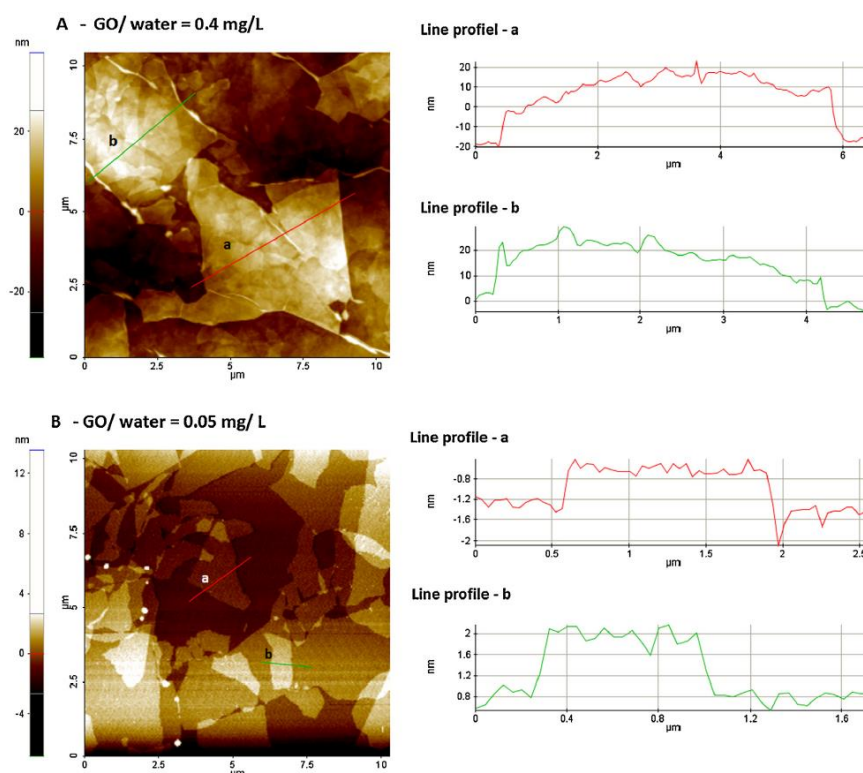


**Figure 9.** Atomic force microscopy (AFM) images and the corresponding line scan profiles of the GO sheets in GO dispersions with different concentrations: (A)  $0.4 \text{ mg L}^{-1}$  and (B)  $0.05 \text{ mg L}^{-1}$ . The ranges of thickness and size of the GO sheets were measured to be 10–20 nm and 3–6 μm in the  $0.4 \text{ mg L}^{-1}$  dispersion and  $\sim 1 \text{ nm}$  and 0.6–1.5 μm in the  $0.05 \text{ mg L}^{-1}$  dispersion. Reproduced from ref. [82], with permission from Elsevier, 2015.

The enhanced hydrophobicity of rGO compared to GO can be attributed to the substitution of the hydrophilic surface functional groups, e.g., carboxylic, hydroxyl, and epoxy groups, by hydrogen atoms. As the reduction process progresses, more and more hydrophilic oxygen-containing surface functional groups would be removed, leaving a hydrophobic basal plane comprised of  $sp^2$  and  $sp^3$  hybridized carbon atoms. A schematic illustration of the changes in surface functional groups of GO during reduction is shown in Figure 10a. As GO nanosheets are deposited on the fabric surface, their hydrophilic edges enriched with oxygen-containing functional groups may form water channels inside the coating layers composed of stacking GO nanosheets, allowing the interlayer transportation of water molecules from the GO coating to the fabric substrate. However, when rGO is used to coat the fabrics instead of GO, the water channels inside the coating layer are blocked due to the depletion of the oxygen-containing functional groups in the edge region of the rGO nanosheets, as shown in Figure 10b. Indeed, the apparent wettability of the GO coating layer can be determined by the edge-to-surface ratios of the GO nanosheets. Intensive water channels can be formed inside the coating layer as small GO nanosheets with high edge-to-surface ratios are used, resulting in a more hydrophilic surface coating. On the other hand, fewer water channels can be formed as large GO nanosheets with low edge-to-surface ratios are used, resulting in more hydrophobic surface coating.

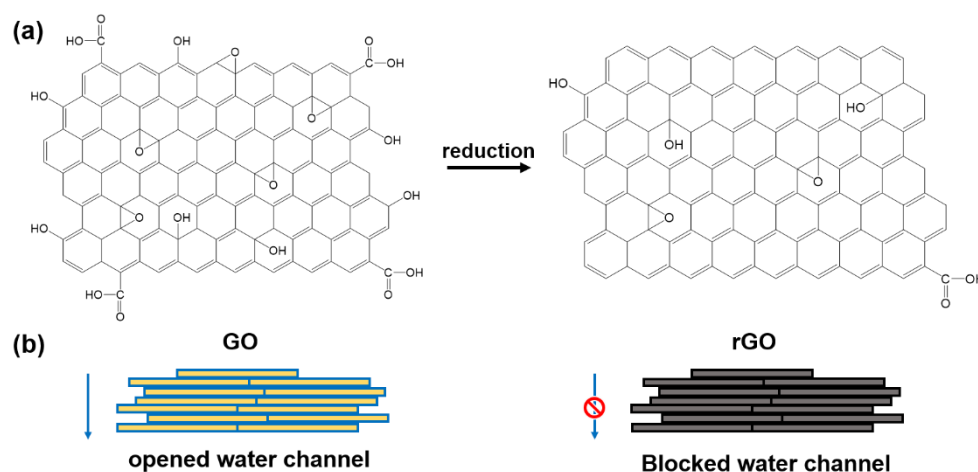


**Figure 10.** (a) Changes in the surface functional groups of GO nanosheets during the reduction process, the major surface functional groups of GO and rGO, are shown, respectively. (b) Schematic illustrations of the opened and blocked water channels formed by the stacking GO and rGO nanosheets.

The hydrophobic rGO can be easily integrated with other functional materials, e.g., nanoparticles, resins, and silanes, to synthesize hybrid coatings on the fabric surface with multi-functionality. For example, T. Makowski et al. have reported the fabrication of superhydrophobic and conductive cotton fabrics by applying an additional coating layer of methyltrichlorosilane (MTCS) on the surface of the rGO-coated cotton fabric [88]. They also discovered that the wettability of the rGO-coated cotton fabric obtained by the thermal reduction process can change from hydrophobic to hydrophilic, depending on the hydrophobicity of the reducing reagents added during the reduction process. X. Zhou et al. have reported the fabrication of  $SiO_2$ /rGO hybrid coating on cotton fabrics by spray-coating the  $SiO_2$ /GO dispersion on one side of the cotton fabric; subsequently, the  $SiO_2$ /GO coating was converted to the  $SiO_2$ /rGO coating by thermal reduction [89]. The integration of  $SiO_2$  nanoparticles with rGO can enhance the hydrophobicity and the thermal insulation property of the coated fabric while the air permeability is not affected. Moreover, K. Chen et al. have reported the fabrication of superhydrophobic, conductive, and self-healing coatings on cotton fabrics by integrating rGO with  $SiO_2$  and polyurethane [90]. According to their method, the  $SiO_2$  nanoparticles were crosslinked by organosilanes and covalently bonded to the amino-pyrene molecules, which can function as the linkers to connect the

silica nanoparticles and rGO together. The SiO<sub>2</sub> nanoparticle-modified rGO was then mixed with the polyurethane resin, and the mixture was applied onto cotton fabrics by rod-coating. Predictable multi-functionality has been achieved for the hybrid coating, as superhydrophobicity was brought by the SiO<sub>2</sub>-modified rGO (Figure 11a,b), conductivity was provided by the rGO (Figure 11c), and self-healing was brought by polyurethane (Figure 11d). Self-healing, conductive, superhydrophobic coating can also be constructed on the cotton fabric surface by integrating rGO with polydopamine (PDA), Cu nanoparticles, and stearic acid [91]. To fabricate the multi-functional coating, cotton fabric was subsequently immersed in the GO/PDA solution, Cu electroless plating solution, and stearic acid emulsion, respectively. The self-healing property of the hybrid coating was brought by PDA, while high conductivity and superhydrophobicity were provided by the synergistic effects of rGO/Cu and rGO/Cu/stearic acid, respectively. By integrating rGO with TiO<sub>2</sub> nanoparticles and polydimethylsiloxane (PDMS), S. Gao et al. have obtained superhydrophobic, conductive, and photoactive coating on cotton fabrics [92]. Hierarchical micro/nano surface structures were formed by the cotton fabric/rGO/TiO<sub>2</sub>-PDMS multilayers, which made the coated fabric superhydrophobic (WCA = 159.3°) and water-repellent; the presence of TiO<sub>2</sub> nanoparticles in the coating made it photoactive and gained the function of photocatalytic degradation of color stains and contaminants under UV radiation. By integrating rGO with the photoactive CuS particles and PDMS, L. Xu et al. have fabricated robust superhydrophobic coating on cotton fabrics with excellent UV protection and photodegradation properties [93]. The rGO and CuS particles were encapsulated by the PDMS matrix, which was strongly adhered to the cotton fabric substrate via covalent bonds. Therefore, the rGO/CuS/PDMS hybrid coating was extremely durable, which can maintain its superhydrophobicity and superlipophilicity after 1000 cycles of abrasion and 96 h of UV radiation and showed a high oil–water separation efficiency. By integrating fluorine-grafted rGO and  $\gamma$ -oxo-1-pyrenebutyric acid, superhydrophobic and superlipophilic hybrid coating was fabricated on the surface of cotton fabrics, polyurethane foams, and polypropylene (PP) membranes, which showed excellent performance in oil–water separation, such as high separation efficiency, high durability, chemical resistance, and anti-fouling property [94].

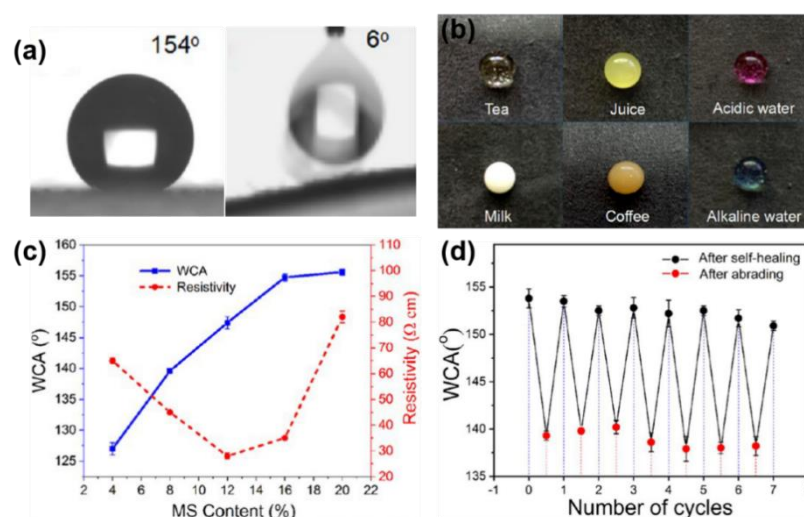


**Figure 11.** The SiO<sub>2</sub>/rGO/polyurethane hybrid coating showed multi-functionality on the cotton fabric, including (a) superhydrophobicity with a high WCA (154°) and low sliding angle (6°); (b) robust water-repellent property that can resist aqueous droplets with different surface tension; (c) correlated superhydrophobicity and conductivity; (d) self-healing properties. Reproduced from ref. [90], with permission from The American Chemical Society, 2022.

In summary, a robust superhydrophobic surface with high water contact angles, low sliding angles, and high durability can be achieved on the fabric surface through

the mechanism of the “lotus effect”. Hierarchical micro-nano surface textures can be constructed on the fabric surface by co-depositing GO or rGO with inorganic nanoparticles, e.g., SiO<sub>2</sub>, TiO<sub>2</sub>, CuS, which may significantly increase the surface roughness; low surface energy coatings, e.g., polyurethane, PDMS, stearic acid, can be applied to immobilize the surface micro-nano textures and synthesize robust superhydrophobic surfaces.

### 3.4. Electromechanical and Sensory Properties

By coating the fabrics with rGO, electrically conductive pathways can be created by the interwoven fibers whose surfaces are covered by the adsorbed rGO nanosheets. However, the apparent conductivities of the coated fabrics are strongly dependent on the applied coating and reduction processes, which may vary case by case. The conductive fabrics can be utilized as flexible, deformable, and sensitive strain sensors that can be conformally attached to the human body and accurately sense the body motions. For example, N. Karim et al. have fabricated rGO-coated cotton fabrics and demonstrated their application as wearable strain sensors [35]. According to their method, rGO was obtained by the chemical reduction of GO by Na<sub>2</sub>S<sub>2</sub>O<sub>4</sub> and NH<sub>3</sub>; the as-obtained rGO was purified by several washing cycles and diluted to make a stable dispersion. Subsequently, the rGO was coated on cotton fabrics by a dip-pad-dry process. A resistivity of 361.82 kΩ/sq was obtained for the rGO-coated cotton fabric prepared by a single dip-pad-dry process, which was insufficient for the wearable sensor application. To increase the conductivity, repeated cycles of the dip-pad-dry process can be applied to the coated fabrics, e.g., the resistivity of the rGO-coated cotton fabric decreased to 36.94 kΩ/sq after five repeated coating cycles, which was suitable for the sensory applications. B. C. Gültekîn has reported the fabrication of the rGO-coated nonwoven cotton fabrics by using a dip-dry process [65]. The cotton fabric was first coated by GO through five repeated dip-dry cycles, and then the GO coating on the fabric was reduced to rGO by Na<sub>2</sub>S<sub>2</sub>O<sub>4</sub>. A resistivity of 1.16 kΩ/sq can be obtained for the as-prepared rGO-coated nonwoven cotton fabric with a basis weight of 40 g m<sup>-2</sup>, which decreased to 0.598 kΩ/sq as the fabric basis weight increased to 70 g m<sup>-2</sup>. U. Mizerska et al. have reported the fabrication of rGO and rGO/organosilicon-coated cotton fabrics with superhydrophobicity and tunable conductivities [85]. The rGO-coated cotton fabric was prepared by a two-step process: (i) the fabric was coated by GO through dipping in the GO dispersion and dried in the ambient condition; the dip-dry process was repeated four times; the GO coated fabric was thermally reduced on a hot stage at 220 °C and cooled down to room temperature. A resistivity of 740 kΩ/sq can be obtained for the as-prepared rGO-coated cotton fabric. Moreover, the resistivity of the rGO-coated fabric increased significantly to 2.7 MΩ/sq upon the incorporation of the organosilicon within the coating dispersion; on the other, the robustness of the superhydrophobicity was remarkably enhanced.

K. Chen et al. have reported the fabrication of a conductive, flexible, and self-healing film by curing the polyurethane resin containing the silica nanoparticle-modified rGO [90]. A resistivity of 34 Ω · cm can be obtained for the composite polyurethane film, which gradually increased as the film went through repeating cut-and-heal cycles. The composite polyurethane film can be coated on a cotton fabric, forming a strain sensor that can be used to sense the finger motions with high sensitivity and repeatability. Y. Ni et al. have reported the fabrication of PDA/rGO/Cu/STA-coated cotton fabric, which showed robust superhydrophobic properties and a high conductivity of 6769 S m<sup>-1</sup> [91]. The coated fabric can be applied as a high-performance underwater strain sensor for sensing different underwater motions. S. Gao et al. have fabricated superhydrophobic, self-cleaning, and conductive PDMS/TiO<sub>2</sub>/rGO coated cotton fabric, showing high sensitivity and repeatability as a strain sensor in detecting various human motions [92]. K. S. Sadanandan et al. have reported the fabrication of rGO-coated fabrics by using the ultrasonic spray coating technique [95]. The commercial rGO suspension was coated on nylon, meta-aramid, and polyester fabrics by three ultrasonic spray coating cycles, forming homogeneous rGO coatings on the fabric surface, and a sheet resistance of 45 kΩ/sq can be obtained for

the rGO-coated nylon fabric. A. Khan et al. have reported the usage of the nanocomposite of rGO, Prussian blue, and graphite/polyurethane paste as the electrode material to fabricate wearable lactate sensors on hydrophobic cotton fabrics [96]. A comprehensive summary of the compositions, fabrication methods, and functional properties of the existing graphene-based coatings on textiles and fabrics is provided in Table 1.

**Table 1.** Summary of the materials, substrates, methods, and functional properties of the graphene-based coatings mentioned in the literature covered in this review.

Coating Materials	Substrates	Coating Methods	Properties			
			Anti-Bacterial Efficiency (%)	UV Protection Factor	WCA	Resistance/Conductivity
rGO [35]	3/1 twill cotton fabric	dip-pad-dry (5 times)	-	-	-	36.94 kΩ/sq
GO [51]	cotton fabric	suction filtration (3 times)	98% ( <i>E. coli</i> )	-	-	-
GO [53]	cotton fabric	dip and dry (3 times)	~70% ( <i>E. coli</i> ); 93% ( <i>S. iniae</i> )	-	-	-
rGO/organosilicon [55]	plain-woven cotton fabric (145 g m <sup>-2</sup> )	dip-pad-dry (4 times); thermal reduction (up to 220 °C)	-	-	162°	8.3 MΩ/sq
rGO/organosilicon/N-octylamine [55]	plain-woven cotton fabric (145 g m <sup>-2</sup> )	dip-pad-dry (4 times); thermal reduction (up to 220 °C)	-	-	150°	290 MΩ/sq
rGO/organosilicon/tert-butylamine [55]	plain-woven cotton fabric (145 g m <sup>-2</sup> )	dip-pad-dry (4 times); thermal reduction (up to 220 °C)	-	-	168°	55 MΩ/sq
rGO/QSA [56]	cotton fabric	dip-dry (10 cycles); chemical reduction dip-dry (10 cycles);	79.89% ( <i>S. aureus</i> ); 64.86% ( <i>E. coli</i> )	346	145.2°	4.4 kΩ/sq
rGO/QSA/Chlorine [56]	cotton fabric	chemical reduction; dip in bleach solution and then dry	100% ( <i>S. aureus</i> ); 100% ( <i>E. coli</i> )	323	153.6°	~350–2500 kΩ/sq
rGO/Cu NPs [57]	cotton fabric	dip coating in GO dispersion; then dip coating in CuCl <sub>2</sub> solution; chemical reduction	99% ( <i>E. coli</i> ); 99% ( <i>C. xerosis</i> ); 99% ( <i>M. luteus</i> )	-	160°	-
rGO/Ag NPs [58]	nonwoven fabric (50% rayon, 50% polyester)	spray coating of GO; electrochemical reduction; electrodeposition of Ag NPs	99.99% ( <i>E. coli</i> )	-	148°	~0.024 S cm <sup>-1</sup>
GO [63]	cotton fabric	dip-dry	95.6% ( <i>E. coli</i> ); 87.6% ( <i>S. aureus</i> )	13.5	-	-
GO/ZnO quantum dots [64]	cotton fabric	dip-pad-dry	-	61.3	-	-
rGO [65]	Cotton spun lace nonwoven fabric (70 g m <sup>-2</sup> )	dip-dry (5 times); chemical reduction	-	167.3	108.2°	598 Ω/sq
rGO [66]	plain-woven polyamide fabric	electrophoretic deposition of GO; thermal reduction (210 °C)	-	>500	96.7°	3.3 S m <sup>-1</sup>
rGO/Cu NPs [67]	plain-woven cotton fabric	dip coating in GO dispersion, then dry (3 times); dip in the CuSO <sub>4</sub> solution and then dry; chemical reduction and thermal treatment	-	46.45	~150°	6.42 kΩ/sq
rGO/Ag NPs [67]	plain-woven cotton fabric	dip coating in GO dispersion, then dry (3 times); dip in the AgNO <sub>3</sub> solution and then dry; chemical reduction and thermal treatment	-	35.31	~150°	52 kΩ/sq
rGO [84]	plain-woven cotton fabric (120 g m <sup>-2</sup> )	dip-dry (3 times); thermal reduction (up to 250 °C)	-	35.8	125°	~10 <sup>4</sup> Ω m <sup>-2</sup>
rGO/organosilicon [85]	plain-woven cotton fabric (145 g m <sup>-2</sup> )	dip-dry (4 times); thermal reduction (up to 220 °C)	-	-	153°	2.7 MΩ/sq
rGO [86]	polyester fabric (110 g m <sup>-2</sup> )	dip-dry; chemical reduction	-	-	123°	1.3 kΩ/sq

Table 1. Cont.

Coating Materials	Substrates	Coating Methods	Properties			
			Anti-Bacterial Efficiency (%)	UV Protection Factor	WCA	Resistance/Conductivity
rGO [88]	plain-woven cotton fabric (~145 g m <sup>-2</sup> )	dip-pad-dry (4 times); and then dip in the Irganox 1010 solution; thermal reduction (up to 220 °C)	-	-	142.4°	3.7 MΩ/sq
rGO/MTCS [88]	plain-woven cotton fabric (~145 g m <sup>-2</sup> )	dip-pad-dry (4 times); and then dip in the Irganox 1010 solution; thermal reduction (up to 220 °C); dip in the MTCS solution	-	-	171.1°	8.3 MΩ/sq
rGO/SiO <sub>2</sub> NPs [89]	plain-woven cotton fabric (~160 g m <sup>-2</sup> )	spray-coating; thermal reduction (180 °C)	-	-	151.4°	-
rGO/SiO <sub>2</sub> NPs/polyurethane [90]	cotton fabric	rod coating and then dry	-	-	153.9°	-
rGO/PDA/Cu NPs/stearic acid [91]	cotton fabric	dip-dry (3 times); chemical reduction; dip in the CuSO <sub>4</sub> solution	-	-	153°	6769 S m <sup>-1</sup>
rGO/PDMS/TiO <sub>2</sub> [92]	plain-woven cotton fabric (~127 g m <sup>-2</sup> )	dip-dry (4 times); dip in the solution of OH-PDMS-OH and Ti(OBu) <sub>4</sub> ; chemical reduction	-	-	159.3°	0.76 kΩ cm <sup>-1</sup>
rGO/CuS/PDMS [93]	cotton fabric	dip-pad-dry-cure	-	851.2	158.4°	-
rGO [95]	polyester fabric	ultrasonic spray coating	-	-	~60°	~120 kΩ/sq
rGO [95]	nylon fabric	ultrasonic spray coating	-	-	~32°	45 kΩ/sq

#### 4. Conclusions

Using the dyeing technique to apply GO coatings onto the fabric is simple, rapid, and green. GO sheets can be conformally deposited on the surface of the fibers and fabrics, showing excellent wash fastness and chemical resistance. Due to its intrinsic chemical functionality, electronic structure, and amphiphilic molecular structure, GO coatings can endow the fabric with applied functions, such as anti-bacterial functions, UV protection, and tunable wettability. Moreover, the intrinsic functions of GO can be enhanced by tuning its size, surface roughness, and functional groups. By reducing GO into rGO, the intrinsic functions, such as conductivity, UV absorption, and hydrophobicity, can be significantly enhanced, which can realize advanced applications, such as E-textiles, UV-protective, and water-repellent clothing. On the other hand, GO and rGO can be easily integrated with other functional materials, formulating hybrid coating solutions for the fabrication of multifunctional fabrics with optimized functional synergy and performance. Metals and their derivatives, silica oxides, organosilanes, and polymers can be integrated with GO and rGO, forming hybrid coatings with predictable and high-performance functions, such as self-cleaning, directional water transport, superhydrophobic and self-healing. Thus, GO can serve as the very base for designing and constructing novel multi-scale, multi-functional, smart textiles with both application and economic significance.

However, the industrial production and commercialization of GO or rGO-coated fabrics may face a few critical challenges. To optimize the applied functions of the GO and rGO-coated fabrics, the effect of post-coating functionalization processes, e.g., chemical reduction, thermal annealing, and resin crosslinking, on the mechanical strength and comfort of the fabric substrate, may need to be analyzed systematically; the fabrication process of the GO and rGO coatings may need to be optimized in order to obtain optimal and consistent loading on the fabric surface. To achieve high loading of GO on the fabric surface, both the fabric surface and the GO surface can be modified to improve the chemical affinity and bonding strength, and the repeatedly dipping and drying cycles can be avoided; the effect of reduction on the physical and chemical properties of the GO coating can be investigated in depth, and the reduction efficiency can be optimized to avoid damaging the fabric substrate; the surface wettability of the GO coated fabric may change from more

hydrophilic to more hydrophobic as GO is converted to rGO, which may induce adverse effects on the subsequent surface modification and functionalization.

**Author Contributions:** Conceptualization, Y.L. and B.F.; writing—original draft preparation, Y.L.; writing—review and editing, B.F.; supervision, J.H.X.; project administration, J.H.X.; funding acquisition, Y.L. and J.H.X. All authors have read and agreed to the published version of the manuscript.

**Funding:** This research was funded by the Natural Science Foundation of China, grant number 81801851.

**Institutional Review Board Statement:** Not applicable.

**Informed Consent Statement:** Not applicable.

**Data Availability Statement:** Not applicable.

**Acknowledgments:** The financial support from Sun Yat-sen University and Hong Kong Polytechnic University is gratefully acknowledged.

**Conflicts of Interest:** The authors declare no conflict of interest.

## References

1. Zhu, Y.; Murali, S.; Cai, W.; Li, X.; Suk, J.W.; Potts, J.R.; Ruoff, R.S. Graphene and graphene oxide: Synthesis, properties, and applications. *Adv. Mater.* **2010**, *22*, 3906–3924. [[CrossRef](#)]
2. Wang, H.; Wang, H.S.; Ma, C.; Chen, L.; Jiang, C.; Chen, C.; Xie, X.; Li, A.; Wang, X. Graphene nanoribbons for quantum electronics. *Nat. Phys.* **2021**, *3*, 791–802. [[CrossRef](#)]
3. Cao, K.; Feng, S.; Han, Y.; Gao, L.; Ly, T.H.; Xu, Z.; Lu, Y. Elastic straining of free-standing monolayer graphene. *Nat. Commun.* **2020**, *11*, 284. [[CrossRef](#)] [[PubMed](#)]
4. Balandin, A.A.; Ghosh, S.; Nika, D.L.; Pokatilov, E.P. Thermal conduction in suspended graphene layers. *Fuller. Nanotub. Carbon Nanostructures* **2010**, *18*, 474–486. [[CrossRef](#)]
5. Dreyer, D.R.; Park, S.; Bielawski, C.W.; Ruoff, R.S. The chemistry of graphene oxide. *Chem. Soc. Rev.* **2010**, *39*, 228–240. [[CrossRef](#)]
6. Chua, C.K.; Pumera, M. Chemical reduction of graphene oxide: A synthetic chemistry viewpoint. *Chem. Soc. Rev.* **2014**, *43*, 291–312. [[CrossRef](#)] [[PubMed](#)]
7. Liu, F.; Wang, C.; Sui, X.; Riaz, M.A.; Xu, M.; Wei, L.; Chen, Y. Synthesis of graphene materials by electrochemical exfoliation: Recent progress and future potential. *Carbon Energy* **2019**, *1*, 173–199. [[CrossRef](#)]
8. Moon, J.; Kim, M.; Kim, S.; Xu, S.; Choi, J.; Whang, D.; Watanabe, K.; Taniguchi, T.; Park, D.S.; Seo, J.; et al. Layer-engineered large-area exfoliation of graphene. *Sci. Adv.* **2020**, *6*, eabc6601. [[CrossRef](#)]
9. Williams, G.; Seger, B.; Kamat, P.V. TiO<sub>2</sub>-graphene nanocomposites. UV-assisted photocatalytic reduction of graphene oxide. *ACS Nano* **2008**, *2*, 1487–1491. [[CrossRef](#)]
10. Ma, H.; Chen, X.; Mohammed, S.; Hu, Y.; Lu, J.; Simon, G.P.; Hou, H.; Wang, H. A thermally reduced graphene oxide membrane interlayered with an in situ synthesized nanospacer for water desalination. *J. Mater. Chem. A* **2020**, *8*, 25951–25958. [[CrossRef](#)]
11. Lin, Y.M.; Garcia, A.V.; Han, S.J.; Farmer, D.B.; Meric, I.; Sun, Y.; Wu, Y.; Dimitrakopoulos, C.; Grill, A.; Avouris, P.; et al. Wafer-scale graphene integrated circuit. *Science* **2011**, *332*, 1294–1297. [[CrossRef](#)]
12. Liu, C.; Chen, Q.; Liu, C.; Zhong, Z. Graphene ambipolar nanoelectronics for high noise rejection amplification. *Nano Lett.* **2016**, *16*, 1064–1068. [[CrossRef](#)] [[PubMed](#)]
13. Bunch, J.S.; Verbridge, S.S.; Alden, J.S.; Zande, A.M.; Parpia, J.M.; Craighead, H.G.; McEuen, P.L. Impermeable atomic membranes from graphene sheets. *Nano Lett.* **2008**, *8*, 2458–2462. [[CrossRef](#)] [[PubMed](#)]
14. Dong, Z.; Jiang, C.; Cheng, H.; Zhao, Y.; Shi, G.; Jiang, L.; Qu, L. Facile fabrication of light, flexible and multifunctional graphene fibers. *Adv. Mater.* **2012**, *24*, 1856–1861. [[CrossRef](#)] [[PubMed](#)]
15. Yu, G.; Hu, L.; Vosgueritchian, M.; Wang, H.; Xie, X.; McDonough, J.R.; Cui, X.; Cui, Y.; Bao, Z. Solution-processed graphene/MnO<sub>2</sub> nanostructured textiles for high-performance electrochemical supercapacitors. *Nano Lett.* **2011**, *11*, 2905–2911. [[CrossRef](#)]
16. Hong, X.; Yu, R.; Hou, M.; Jin, Z.; Dong, Y.; Zhu, C.; Wan, J.; Li, Y. Smart fabric strain sensor comprising reduced graphene oxide with structure-based negative piezoresistivity. *J. Mater. Sci.* **2021**, *56*, 16946–16962. [[CrossRef](#)]
17. Lerf, A.; He, H.; Forster, M.; Klinowski, J. Structure of graphene oxide revisited. *J. Phys. Chem. B* **1998**, *102*, 4477–4482. [[CrossRef](#)]
18. Kim, J.; Cote, L.J.; Kim, F.; Yuan, W.; Shull, K.R.; Huang, J. Graphene oxide sheets at interfaces. *J. Am. Chem. Soc.* **2010**, *132*, 8180–8186. [[CrossRef](#)]
19. Withers, N. Surfactant sheets. *Nat. Chem.* **2010**. [[CrossRef](#)]
20. Luo, J.; Yang, L.; Sun, D.; Gao, Z.; Jiao, K.; Zhang, J. Graphene oxide “surfactant”-directed tunable concentration of graphene dispersion. *Small* **2020**, *16*, 2003426. [[CrossRef](#)]
21. Wang, S.; Chia, P.J.; Chua, L.L.; Zhao, L.H.; Png, R.Q.; Sivaramakrishnan, S.; Zhou, M.; Goh, R.G.S.; Friend, R.H.; Wee, A.T.S.; et al. Band-like transport in surface-functionalized highly solution-processable graphene nanosheets. *Adv. Mater.* **2008**, *20*, 3440–3446. [[CrossRef](#)]

22. Li, B.; Hou, W.; Sun, J.; Jiang, S.; Xu, L.; Li, G.; Memon, M.A.; Cao, J.; Huang, Y.; Bielawski, C.W.; et al. Tunable functionalization of graphene oxide sheets through surface-initiated cationic polymerization. *Macromolecules* **2015**, *48*, 994–1001. [[CrossRef](#)]
23. Guo, S.; Garaj, S.; Bianco, A.; Ménard-Moyon, C. Controlling covalent chemistry on graphene oxide. *Nat. Rev. Phys.* **2022**, *4*, 247–262. [[CrossRef](#)]
24. Aujara, K.M.; Chieng, B.W.; Ibrahim, N.A.; Zainuddin, N.; Ratnam, C.T. Gamma-irradiation induced functionalization of graphene oxide with organosilanes. *Int. J. Mol. Sci.* **2019**, *20*, 1910. [[CrossRef](#)] [[PubMed](#)]
25. Pyun, J. Graphene oxide as catalyst: Application of carbon materials beyond nanotechnology. *Angew. Chem. Int. Ed.* **2011**, *50*, 46–48. [[CrossRef](#)]
26. Sharma, N.; Swami, S.; Shrivastava, V.; Nair, R.; Shrivastava, R. Graphene oxide and functionalized graphene oxide: Robust, 2D material as heterogeneous green catalyst for heterocyclic synthesis. *Mater. Today Proc.* **2021**, *43*, 3309–3317. [[CrossRef](#)]
27. Yuan, S.; Wang, J.; Mei, J.; Zhao, J.; Huang, G.; Li, Z.; He, X.; Fan, J. Fabric comprised of cotton impregnated with graphene oxide and coated with polystyrene for personal moisture and thermal management. *ACS Appl. Nano Mater.* **2023**, *6*, 4499–4510. [[CrossRef](#)]
28. Zhou, J.; Luo, Q.; Gao, P.; Ma, H. Assembly of graphene oxide on cotton fiber through dyeing and their properties. *RSC Adv.* **2020**, *10*, 11982–11989. [[CrossRef](#)]
29. Khoso, N.A.; Xu, G.; Xie, J.; Sun, T.; Wang, J. The fabrication of a graphene and conductive polymer nanocomposite-coated highly flexible and washable woven thermoelectric nanogenerator. *Mater. Adv.* **2021**, *2*, 3695–3704. [[CrossRef](#)]
30. Shathi, M.A.; Chen, M.; Khoso, N.A.; Rahman, M.T.; Bhattacharjee, B. Graphene coated textile based highly flexible and washable sports bra for human health monitoring. *Mater. Des.* **2020**, *193*, 108792. [[CrossRef](#)]
31. Yang, S.; Sha, S.; Lu, H.; Wu, J.; Ma, J.; Wang, D.; Hou, C.; Sheng, Z. Graphene oxide and reduced graphene oxide coated cotton fabrics with opposite wettability for continuous oil/water separation. *Sep. Purif. Technol.* **2021**, *259*, 118095. [[CrossRef](#)]
32. Shateri-Khalilabad, M.; Yazdanshenas, M.E. Fabricating electroconductive cotton textiles using graphene. *Carbohydr. Polym.* **2013**, *96*, 190–195. [[CrossRef](#)] [[PubMed](#)]
33. Chen, F.; Liu, H.; Xu, M.; Ye, J.; Li, Z.; Qin, L.; Zhang, T. Flexible cotton fabric with stable conductive coatings for piezoresistive sensors. *Cellulose* **2021**, *28*, 10025–10038. [[CrossRef](#)]
34. Shateri-Khalilabad, M.; Yazdanshenas, M.E. Preparation of superhydrophobic electroconductive graphene-coated cotton cellulose. *Cellulose* **2013**, *20*, 963–972. [[CrossRef](#)]
35. Karim, N.; Afroj, S.; Tan, S.; He, P.; Fernando, A.; Carr, C.; Novoselov, K.S. Scalable production of graphene-based wearable E-Textiles. *ACS Nano* **2017**, *11*, 12266–12275. [[CrossRef](#)]
36. Fugetsu, B.; Sano, E.; Yu, H.; Mori, K.; Tanaka, T. aoxide as dyestuffs for the creation of electrically conductive fabrics. *Carbon* **2010**, *48*, 3340–3345. [[CrossRef](#)]
37. Krishnamoorthy, K.; Navaneethaiyer, U.; Mohan, R.; Lee, J.; Kim, S. Graphene oxide nanostructures modified multifunctional cotton fabrics. *Appl. Nanosci.* **2012**, *2*, 119–216. [[CrossRef](#)]
38. Molina, J.; Fernandez, J.; Rio, A.I.; Bonastre, J.; Cases, F. Chemical and electrochemical study of fabrics coated with reduced graphene oxide. *Appl. Surf. Sci.* **2013**, *279*, 46–54. [[CrossRef](#)]
39. Yang, F.; Lan, C.; Zhang, H.; Guan, J.; Zhang, F.; Fei, B.; Zhang, J. Study on graphene/CNC-coated bamboo pulp fabric: Preparation of fabrics with thermal conductivity. *Polymers* **2019**, *11*, 1265. [[CrossRef](#)]
40. Yun, Y.J.; Hong, W.G.; Kim, W.; Jun, Y.; Kim, B.H. A novel method for applying reduced graphene oxide directly to electronic textiles from yarns to fabrics. *Adv. Mater.* **2013**, *25*, 5701–5705. [[CrossRef](#)]
41. Khoso, N.A.; Xie, J.; Xu, G.; Sun, T.; Wang, J. Enhanced thermoelectric performance of graphene based nanocomposite coated self-powered wearable e-textiles for energy harvesting from human body heat. *RSC Adv.* **2021**, *11*, 16675–16687. [[CrossRef](#)] [[PubMed](#)]
42. Kumar, A.; Kebaili, I.; Boukhris, I.; Vaish, R.; Kumar, A.; Park, H.K.B.; Joo, Y.H.; Sung, T.H. Cotton functionalized with polyethylene glycol and graphene oxide for dual thermoregulating and UV-protection applications. *Sci. Rep.* **2023**, *13*, 5923. [[CrossRef](#)]
43. Manasoglu, G.; Celen, R.; Kanik, M.; Ulcay, Y. Electrical resistivity and thermal conductivity properties of graphene-coated woven fabrics. *J. Appl. Polym. Sci.* **2019**, *136*, 48024. [[CrossRef](#)]
44. Hunter, C.A.; Sanders, J.K.M. The nature of  $\pi$ - $\pi$  interactions. *J. Am. Chem. Soc.* **1990**, *112*, 5525–5534. [[CrossRef](#)]
45. Farouk, A.; Saeed, S.E.; Sharaf, S.; El-Hady, M.M.A. Photocatalytic activity and antibacterial properties of linen fabric using reduced graphene oxide/silver nanocomposite. *RSC Adv.* **2020**, *10*, 41600–41611. [[CrossRef](#)]
46. Pedrosa, M.; Sampaio, M.J.; Horvat, T.; Nunes, O.C.; Dražić, G.; Rodrigues, A.E.; Figueiredo, J.L.; Silva, C.G.; Silva, A.M.T.; Faria, J.L. Visible-light-induced self-cleaning functional fabrics using graphene oxide/carbon nitride materials. *Appl. Surf. Sci.* **2019**, *497*, 143757. [[CrossRef](#)]
47. Gong, T.; Kim, J.; Woo, J.Y.; Jang, J.; Lee, S.E.; Han, C. Fabrics coated with hot-iron-treated graphene oxide for a self-cleaning and mechanically robust water-oil separation material. *RSC Adv.* **2017**, *7*, 25796–25802. [[CrossRef](#)]
48. Rafiee, J.; Rafiee, M.A.; Yu, Z.; Koratkar, N. Superhydrophobic to superhydrophilic wetting control in graphene films. *Adv. Mater.* **2010**, *22*, 2151–2154. [[CrossRef](#)]
49. Liu, Y.; Wang, X.; Fei, B.; Hu, H.; Lai, C.; Xin, J.H. Bioinspired, stimuli-responsive, multifunctional superhydrophobic surface with directional wetting, adhesion, and transport of water. *Adv. Funct. Mater.* **2015**, *25*, 5047–5056. [[CrossRef](#)]

50. Liu, S.; Zeng, T.H.; Hofmann, M.; Burcombe, E.; Wei, J.; Jiang, R.; Kong, J.; Chen, Y. Antibacterial activity of graphite, graphite oxide, graphene oxide, and reduced graphene oxide: Membrane and oxidative stresses. *ACS Nano* **2011**, *5*, 6971–6980. [[CrossRef](#)]
51. Zhao, J.; Deng, B.; Lv, M.; Li, J.; Zhang, Y.; Jiang, H.; Peng, C.; Li, J.; Shi, J.; Huang, Q.; et al. Graphene-oxide based antibacterial cotton fabrics. *Adv. Healthc. Mater.* **2013**, *2*, 1259–1266. [[CrossRef](#)]
52. Liu, Y.; Wang, X.; Qi, K.; Xin, J.H. Functionalization of cotton with carbon nanotubes. *J. Mater. Chem.* **2008**, *18*, 3454–3460. [[CrossRef](#)]
53. Yaghoubidoust, F.; Salimi, E. A simple method for the preparation of antibacterial cotton fabrics by coating graphene oxide nanosheets. *Fibers Polym.* **2019**, *20*, 1155–1160. [[CrossRef](#)]
54. Yadav, N.; Dubey, A.; Shukla, S.; Saini, C.P.; Gupta, G.; Priyadarshini, R.; Lochab, B. Graphene oxide-coated surface: Inhibition of bacterial biofilm formation due to specific surface-interface interactions. *ACS Omega* **2017**, *2*, 3070–3082. [[CrossRef](#)] [[PubMed](#)]
55. Mizerska, U.; Fortuniak, W.; Makowski, T.; Svyntkivska, M.; Piorkowska, E.; Kowalczyk, D.; Brzezinski, S.; Kregiel, D. Antibacterial electroconductive rGO modified cotton fabric. *Polym. Adv. Technol.* **2021**, *32*, 3975–3981. [[CrossRef](#)]
56. Xu, Z.; Pan, N.; Xue, Y.; Jiang, T.; Wang, Y. Long-lasting renewable antibacterial graphene/N-halamine-coated cotton fabrics benefiting from enhanced UV stability and quantitative tracking of bactericidal factors. *Int. J. Biol. Macromol.* **2022**, *222*, 1192–1200. [[CrossRef](#)]
57. Kim, J.; Kang, S.H.; Choi, Y.; Lee, W.; Kim, N.; Tanaka, M.; Kang, S.H.; Choi, J. Antibacterial and biofilm-inhibiting cotton fabrics decorated with copper nanoparticles grown on graphene nanosheets. *Sci. Rep.* **2023**, *13*, 11947. [[CrossRef](#)] [[PubMed](#)]
58. Jafari, B.; Lacerda, C.M.R.; Botte, G.G. Facile electrochemical preparation of hydrophobic antibacterial fabrics using reduced graphene oxide/silver nanoparticles. *ChemElectroChem* **2023**, *10*, e202201111. [[CrossRef](#)]
59. Rodrigues, D.P.; Moreirinha, C.; Rajan, G.; Neves, A.I.S.; Freitas, S.C.; Sequeira, S.; Russo, S.; Craciun, M.F.; Almeida, A.; Alves, H. Conversion of antibacterial activity of graphene-coated textiles through surface polarity. *Nano Sel.* **2023**, *4*, 463–524. [[CrossRef](#)]
60. Abdolkarimi-Mahabadi, M.; Bayat, A.; Mohammadi, A. Use of UV-vis spectrophotometry for characterization of carbon nanostructures: A review. *Theor. Exp. Chem.* **2021**, *57*, 191–198. [[CrossRef](#)]
61. Senthil, R.A.; Selvi, A.; Arunachalam, P.; Amudha, L.S.; Madhavan, J.; Al-Mayouf, A.M. A sensitive electrochemical detection of hydroquinone using newly synthesized  $\alpha$ -Fe<sub>2</sub>O<sub>3</sub>-graphene oxide nanocomposite as an electrode material. *J. Mater. Sci.* **2017**, *28*, 10081–10091. [[CrossRef](#)]
62. Johra, F.T.; Lee, J.; Jung, W. Facile and safe graphene preparation on solution based platform. *J. Ind. Eng. Chem.* **2014**, *20*, 2883–2887. [[CrossRef](#)]
63. He, X.; Liu, Q.; Zhou, Y.; Chen, Z.; Zhu, C.; Jin, W. Graphene oxide-silver/cotton fiber fabric with anti-bacterial and anti-UV properties for wearable gas sensors. *Front. Mater. Sci.* **2021**, *15*, 406–415. [[CrossRef](#)]
64. Zuo, D.; Li, G.; Ling, Y.; Cheng, S.; Xu, J.; Zhang, H. Durable UV-blocking property of cotton fabrics with nanocomposite coating based on graphene oxide/ZnO quantum dot via water-based self-assembly. *Fibers Polym.* **2021**, *22*, 1837–1843. [[CrossRef](#)]
65. Gültek, B.C. Electrically conductive, hydrophobic, UV protective and lightweight cotton spunlace nonwoven fabric coated with reduced graphene oxide. *Turk. J. Chem.* **2022**, *46*, 968–986. [[CrossRef](#)]
66. Zhao, H.; Tian, M.; Hao, Y.; Qu, L.; Zhu, S.; Chen, S. Fast and facile graphene oxide grafting on hydrophobic polyamide fabric via electrophoretic deposition route. *J. Mater. Sci.* **2018**, *53*, 9504–9520. [[CrossRef](#)]
67. Bhattacharjee, S.; Macintyre, C.R.; Wen, X.; Bahl, P.; Kumar, U.; Chughtai, A.A.; Joshi, R. Nanoparticles incorporated graphene-based durable cotton fabrics. *Carbon* **2020**, *166*, 148–163. [[CrossRef](#)]
68. Xiang, Q.; Yu, J.; Jaroniec, M. Graphene-based semiconductor photocatalysts. *Chem. Soc. Rev.* **2012**, *41*, 782–796. [[CrossRef](#)]
69. Liao, G.; Chen, S.; Quan, X.; Yu, H.; Zhao, H. Graphene oxide modified g-C<sub>3</sub>N<sub>4</sub> hybrid with enhanced photocatalytic capability under visible light irradiation. *J. Mater. Chem.* **2012**, *22*, 2721–2726. [[CrossRef](#)]
70. Kuang, Y.; Shang, J.; Zhu, T. Photoactivated graphene oxide to enhance photocatalytic reduction of CO<sub>2</sub>. *ACS Appl. Mater. Interfaces* **2020**, *12*, 3580–3591. [[CrossRef](#)] [[PubMed](#)]
71. Prasad, C.; Liu, Q.; Tang, H.; Yuvaraja, G.; Long, J.; Rammohan, A.; Zyryanov, G.V. An overview of graphene oxide supported semiconductors based photocatalysts: Properties, synthesis and photocatalytic applications. *J. Mol. Liq.* **2020**, *297*, 111826. [[CrossRef](#)]
72. Yeh, T.F.; Cihlar, J.; Chang, C.Y.; Cheng, C.; Teng, H. Roles of graphene oxide in photocatalytic water splitting. *Mater. Today* **2013**, *16*, 78–84. [[CrossRef](#)]
73. Zhang, J.; Liu, K.; Sun, S.; Sun, R.; Ma, J. Photo-splitting xylose and xylan to xylonic acid and carbon monoxide. *Green Chem.* **2022**, *24*, 8367–8376. [[CrossRef](#)]
74. Yang, X.; Qin, J.; Jiang, Y.; Chen, K.; Yan, X.; Zhang, D.; Li, R.; Tang, H. Fabrication of P25/Ag<sub>3</sub>PO<sub>4</sub>/graphene oxide heterostructures for enhanced solar photocatalytic degradation of organic pollutants and bacteria. *Appl. Catal. B* **2015**, *166–167*, 231–240. [[CrossRef](#)]
75. Liu, X.; Ma, R.; Wang, X.; Ma, Y.; Yang, Y.; Zhuang, L.; Zhang, S.; Jehan, R.; Chen, J.; Wang, X. Graphene oxide-based materials for efficient removal of heavy metal ions from aqueous solution: A review. *Environ. Pollut.* **2019**, *252*, 62–73. [[CrossRef](#)] [[PubMed](#)]
76. Qian, D.; Chen, D.; Li, N.; Xu, Q.; Li, H.; He, J.; Lu, J. TiO<sub>2</sub>/sulfonated graphene oxide/Ag nanoparticle membrane: In situ separation and photodegradation of oil/water emulsions. *J. Membr. Sci.* **2018**, *554*, 16–25. [[CrossRef](#)]
77. Yaqoob, A.A.; Noor, N.H.M.; Umar, K.; Adnan, R.; Ibrahim, M.N.M.; Rashid, M. Graphene oxide-ZnO nanocomposite: An efficient visible light photocatalyst for degradation of rhodamine B. *Appl. Nanosci.* **2021**, *11*, 1291–1302. [[CrossRef](#)]

78. Sangermano, M.; Calza, P.; Lopez-Manchado, M.A. Graphene oxide-epoxy hybrid material as innovative photocatalyst. *J. Mater. Sci.* **2013**, *48*, 5204–5208. [[CrossRef](#)]
79. Lu, K.Q.; Li, Y.H.; Tang, Z.R.; Xu, Y.J. Roles of graphene oxide in heterogeneous photocatalysis. *ACS Mater. Au* **2021**, *1*, 37–54. [[CrossRef](#)]
80. Qiu, R.; Yuan, S.; Xiao, J.; Chen, X.D.; Selomulya, C.; Zhang, X.; Woo, M.W. Effects of edge functional groups on water transport in graphene oxide membranes. *ACS Appl. Mater. Interfaces* **2019**, *11*, 8483–8491. [[CrossRef](#)]
81. Brakat, A.; Zhu, H. Nanocellulose-graphene hybrids: Advanced functional materials as multifunctional sensing platform. *Nano-Micro Lett.* **2021**, *13*, 94. [[CrossRef](#)]
82. Tissera, N.D.; Wijesena, R.N.; Perera, J.R.; Silva, K.M.N.; Amaratunge, G.A.J. Hydrophobic cotton textile surfaces using an amphiphilic graphene oxide (GO) coating. *Appl. Surf. Sci.* **2015**, *324*, 455–463. [[CrossRef](#)]
83. Liu, Y.; Wang, B.; Wang, Y.; Chen, J.; Cui, B.; Yin, P.; Chen, J.; Zhang, X.; Zhang, L.; Xin, J.H. Bioinspired superhydrophobic surface constructed from hydrophilic building blocks: A case study of core-shell polypyrrole-coated copper nanoneedles. *Coatings* **2020**, *10*, 347. [[CrossRef](#)]
84. Cai, G.; Xu, Z.; Yang, M.; Tang, B.; Wang, X. Functionalization of cotton fabrics through thermal reduction of graphene oxide. *Appl. Surf. Sci.* **2017**, *393*, 441–448. [[CrossRef](#)]
85. Mizerska, U.; Fortuniak, W.; Makowski, T.; Svyntkivska, M.; Piorkowska, E.; Kowalczyk, D.; Brzezinski, S. Electrically conductive and hydrophobic rGO-containing organosilicon coating of cotton fabric. *Prog. Org. Coat.* **2019**, *137*, 105312. [[CrossRef](#)]
86. Berendjchi, A.; Khajavi, R.; Yousefi, A.A.; Yazdanshenas, M.E. Surface characteristics of coated polyester fabric with reduced graphene oxide and polypyrrole. *Appl. Surf. Sci.* **2016**, *367*, 36–42. [[CrossRef](#)]
87. Jishnu, A.; Jayan, J.S.; Saritha, A.; Sethulekshmi, A.S.; Venu, G. Superhydrophobic graphene-based materials with self-cleaning and anticorrosion performance: An appraisal of neoteric advancement and future perspectives. *Colloids Surf. A* **2020**, *606*, 125395.
88. Makowski, T.; Svyntkivska, M.; Piorkowska, E.; Mizerska, U.; Fortuniak, W.; Kowalczyk, D.; Brzezinski, S. Conductive and superhydrophobic cotton fabric through pentaerythritol tetrakis(3-(3,5-di-tert-butyl-4-hydroxyphenyl)propionate) assisted thermal reduction of graphene oxide and modification with methyltrichlorosilane. *Cellulose* **2018**, *25*, 5377–5388. [[CrossRef](#)]
89. Zhou, X.; Song, W.; Zhu, G. A facile approach for fabricating silica dioxide/reduced graphene oxide coated cotton fabrics with multifunctional properties. *Cellulose* **2020**, *27*, 2927–2938. [[CrossRef](#)]
90. Chen, K.; Liu, H.; Zhou, J.; Sun, Y.; Yu, K. Polyurethane blended with silica-nanoparticle-modified graphene as a flexible and superhydrophobic conductive coating with a self-healing ability for sensing applications. *ACS Appl. Nano Mater.* **2022**, *5*, 615–625. [[CrossRef](#)]
91. Ni, Y.; Huang, J.; Li, S.; Wang, X.; Liu, L.; Wang, M.; Chen, Z.; Li, X.; Lai, Y. Underwater, multifunctional superhydrophobic sensor for human motion detection. *ACS Appl. Mater. Interfaces* **2021**, *13*, 4740–4749. [[CrossRef](#)] [[PubMed](#)]
92. Gao, S.; Li, H.; Zheng, L.; Huang, W.; Chen, B.; Lai, X.; Zeng, X. Superhydrophobic and conductive polydimethylsiloxane/titanium dioxide @ reduced graphene oxide coated cotton fabric for human motion detection. *Cellulose* **2021**, *28*, 7373–7388. [[CrossRef](#)]
93. Xu, L.; Li, J.; Pan, H.; Wang, L.; Liu, Y.; Shen, Y. Preparation of superhydrophobic cotton fabric with ultraviolet resistance and photocatalysis based on CuS/reduced graphene oxide. *ChemistrySelect* **2023**, *8*, e202300167. [[CrossRef](#)]
94. Guo, G.; Liu, L.; Zhang, Q.; Pan, C.; Zou, Q. Solution-processable, durable, scalable, fluorine-grafted graphene-based superhydrophobic coating for highly efficient oil/water separation under harsh environment. *New J. Chem.* **2018**, *42*, 3819. [[CrossRef](#)]
95. Sadanandan, K.S.; Bacon, A.; Shin, D.W.; Alkhalifa, S.F.R.; Russo, S.; Craciun, M.F.; Neves, A.I.S. Graphene coated fabrics by ultrasonic spray coating for wearable electronics and smart textiles. *J. Phys. Mater.* **2021**, *4*, 014004. [[CrossRef](#)]
96. Khan, A.; Winder, M.; Hossain, G. Modified graphene-based nanocomposite material for smart textile biosensor to detect lactate from human sweat. *Biosens. Bioelectron. X* **2022**, *10*, 100103. [[CrossRef](#)]

**Disclaimer/Publisher’s Note:** The statements, opinions and data contained in all publications are solely those of the individual author(s) and contributor(s) and not of MDPI and/or the editor(s). MDPI and/or the editor(s) disclaim responsibility for any injury to people or property resulting from any ideas, methods, instructions or products referred to in the content.